

Chapter 16

Biomedical Imaging

Emma MacPherson

Abstract This chapter builds on the basic principles of THz spectroscopy and explains how they can be applied to biomedical systems as well as the motivation for doing so. Sample preparation techniques and measurement methods for biomedical samples are described in detail. Examples of medical applications investigated hitherto including breast cancer and skin cancer are also presented.

16.1 Why Is Terahertz Radiation Suitable for Investigating Biomedical Systems?

16.1.1 Safety

The energy of a photon at 1 THz, through Plank's law, $\text{Energy} = hf$, where h is Plank's constant, is equal to 6.6×10^{-22} J or 4.1 meV. The energy needed to ionize an atom is of the order 1,000 times higher than this. For example, the ionization energy of sodium is 5.1 eV. Therefore, the energy of THz light is far too low to cause ionization and is safe from this perspective. Additionally, the power levels used in most systems are less than 1 μW which is a million times lower than the THz radiation naturally emitted by the human body (1 W). This means that thermal effects are negligible. Whether there are any non-thermal effects that could potentially cause cell damage at low powers is a current topic of investigation, but hitherto there is no evidence for concern. Research into safe levels of exposure has been carried out through studies on keratinocytes [1] and blood leukocytes [2] with no adverse effects found. Therefore, it is reasonable to conclude that THz light is safe for probing biological samples at

E. MacPherson (✉)
Electronic and Computer Engineering,
The Hong Kong University of Science and Technology,
Clear Water Bay, Hong Kong, China
e-mail: e.pickwell.97@cantab.net

such power levels and many research groups are keen to investigate its potential for medical applications.

16.1.2 Sensitivity toward Intermolecular Interactions

Although safety is always a primary concern, it is also important that we have more reason to investigate other than that it is safe. After all, poking a sample with a stick might well be safe, but it would not tell us anything useful! So, why is it thought that THz light might be a useful technique to investigate biological samples? The answer lies in the fundamental fact that there are intermolecular vibrations with resonances at THz frequencies. These intermolecular interactions have weak, low energy vibrations with broad features that relate to molecular structure. As discussed earlier, there are strong water absorptions at THz frequencies due to hydrogen bonds. Thus, small changes in water content of tissues can be detected using THz light. This is relevant to applications such as cancer diagnosis as the presence of tumor often increases the blood flow, and thus water content within the tissue. Tumor also disrupts the normal tissue matrix on a cellular level. THz imaging is also sensitive to these changes in structure on a macroscopic level and it has been shown that, in addition to water, structural changes contribute significantly to the differences between THz properties of diseased and healthy tissues [4]. Changes in tissue structure are likely to be caused by cross-linking of proteins. Therefore, since THz spectroscopy of proteins is able to show characteristic features, it is likely that THz spectroscopy of biological samples will also provide useful information.

16.2 Sample Preparation

Many THz researchers come from a science or engineering background and have no previous experience in preparing biomedical samples. Collaborations with medical practitioners will help you learn about the samples you are investigating, health and safety, and ethical considerations but they will not necessarily help you to establish a rigorous experimental protocol. The details below highlight aspects that should be considered before embarking on any measurements of biological samples.

16.2.1 Tissue (de)hydration

Since THz light is very sensitive to water content, small changes in the water content of the sample will affect the resulting THz properties of the sample. For instance, if the sample is an excised piece of tissue, once it has been removed, if it is simply left out in the air it will lose water due to evaporation. Therefore, great care must be

taken to preserve the sample such that it does not become dehydrated. If meaningful comparisons between samples are to be drawn, then the samples must have been prepared and handled identically. For instance, they must be stored in the same type of sample holder, kept at the same temperature and humidity and measured at the same time relative to excision.

Sample size and shape is also important—ideally excised samples should be approximately the same size and shape from the beginning so that all samples will be affected in the same way by the environmental factors. This is because the surface area to volume ratio will affect the tissue—clearly tissue from the center of a $1\text{ cm} \times 1\text{ cm} \times 1\text{ cm}$ sample will have become more dehydrated than tissue from the center of a $2\text{ cm} \times 2\text{ cm} \times 2\text{ cm}$ sample. Ideally, it is good to have a large sample excised initially and then take a small slice of the sample from the middle for measurement.

16.2.2 Repeatability

With all tissue samples, it is important to take several measurements. For instance, it is much better to scan a sample such that an area of the sample is measured rather than a single point measurement being made. Additionally, it is necessary to measure several samples harvested from either the same patient or preferably other patients. Since biological samples have natural variation, as much data as possible should be acquired such that average properties can be calculated along with estimations of the errors.

16.2.3 Example Checklist

The key point is to be consistent and, as standard good experimental practice, record all variables. The most tricky part is often determining all the variables as with biological samples there are lots of them! Table 16.1 is an example checklist, it is by no means an exhaustive list, rather, it is designed to help you identify the variables for your case.

16.3 Systems for Samples

The type of sample you are able to obtain and what you want to find out about the sample will determine how you should perform the THz measurement and the type/geometry of THz system you use.

Table 16.1 Checklist for sample and measurement parameters

Variable	Sample 1	Sample 2
Sample details: species, age, gender, healthy...		
Date and time of sample excision		
Humidity and temperature at excision		
Description of sample storage		
Storage humidity and temperature		
Dimensions of excised sample		
Dimensions of sample measured		
Date and time of sample measurement		
Humidity and temperature during measurement		
Filename where data saved		

16.3.1 *Thin Versus Thick*

If the sample is thick (greater than 500 μm) then due to the typically high attenuation of biological tissues it is unlikely that THz light would be able to pass through it and be detected above the noise in a transmission geometry. So, a reflection geometry system should be used. In this case, only information about the surface of the sample will be obtained.

If the sample is thinner than 500 μm then a transmission geometry should be suitable. It is often better to cut samples into thinner slices e.g., 100–300 μm so that the transmitted THz signal is significantly above the noise floor. However, if the sample is too thin, then unwanted etalon effects will be introduced (Fig. 16.1).

16.3.2 *Homogenous Versus Inhomogenous*

If the sample is homogenous then the refractive index and absorption coefficient can be extracted in either reflection or transmission geometry setups. However, if the sample is inhomogenous then this will be more difficult. It may be useful to image an area of the sample and compare the THz data with histology results to identify regions of tissue types, and then group the data such that the THz spectroscopic properties can be obtained.

Occasionally, it is useful to just look at the reflected/transmitted intensity off/through a sample. If this is the case, a continuous wave (CW) THz system might be able to provide sufficient information. However, CW systems have a narrow fre-

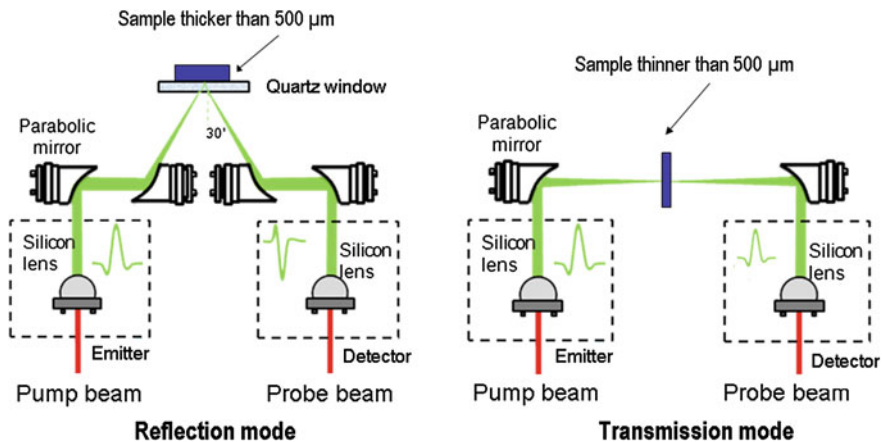


Fig. 16.1 Schematic diagrams to illustrate that biological samples thicker than 500 μm should be measured in reflection geometry and samples thinner than 500 μm should be measured in transmission geometry

quency output and so contrast will only be seen between tissues if their properties at the chosen frequency output are different. Since the area of THz biomedical spectroscopy is relatively new, most studies use a pulsed THz system (which produces broad band THz radiation) so that the frequency dependent properties of the sample can be determined.

16.3.3 Bandwidth and Axial Resolution

As well as determining the frequency range over which the sample can be characterized, the bandwidth of the terahertz system also influences the axial resolution. For a reflection geometry system the axial resolution is given by the coherence length, L_C :

$$L_C = c/2n\Delta f \tag{16.1}$$

where c is the speed of light, n is the refractive index of the sample and Δf is the bandwidth. Therefore, when the bandwidth is increased for a given refractive index, smaller features will be able to be resolved.

The example THz power spectrum in Fig. 16.2 (measured by placing a mirror where the sample should go) starts to fall off at 2 THz resulting in a usable bandwidth of about 1.9 THz.

One problem for biological tissues in particular is that the absorption coefficient of most tissues increases with increasing frequency. For example, the absorption coefficients for water, healthy breast tissue and adipose fat are plotted in Fig. 16.3.

Fig. 16.2 Example THz power spectrum. The maximum usable frequency range for this system is from 0.1 to 2 THz

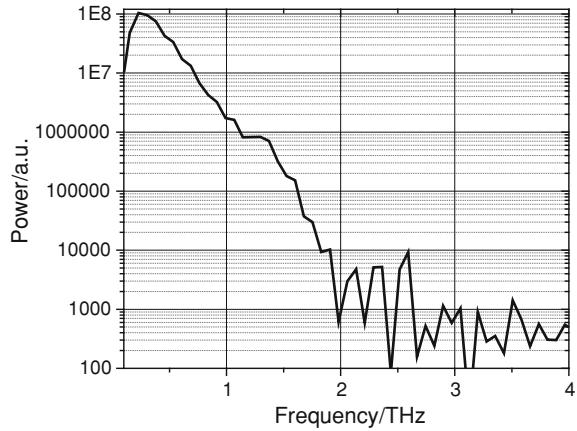
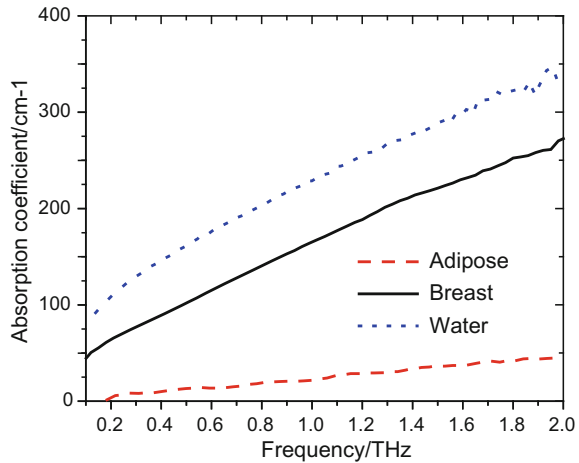


Fig. 16.3 The absorption coefficients for water, healthy breast tissue, and adipose tissue. Data were acquired in transmission geometry



This compounds the signal power roll-off and means that it is even more difficult to achieve high resolution in biological samples.

16.3.4 Signal to Noise Ratio and Penetration Depth

The detectable penetration depth of the terahertz light depends on the attenuation of the sample and also the signal to noise ratio (SNR) of the terahertz signal. For light propagating distance z through a medium with absorption coefficient α , the amplitude A_z is given by:

$$A_z = A_0 e^{-\frac{\alpha}{2}z} \tag{16.2}$$

where A_0 is the initial signal amplitude. Therefore, the furthest distance that THz light can travel in the medium and still be detectable is when:

$$\frac{A_z}{A_0} = \frac{1}{\text{SNR}} \quad (16.3)$$

which means:

$$\ln\left(\frac{A_z}{A_0}\right) = -\ln(\text{SNR}) = -\frac{\alpha}{2}z \quad (16.4)$$

Therefore, the maximum detectable penetration depth is:

$$z = \frac{2}{\alpha} \ln(\text{SNR}) \quad (16.5)$$

If the THz signal is being detected in a reflection geometry then the depth, d into the tissue will be half the distance traveled (assuming normal incidence). Therefore, the maximum penetration depth detectable in a reflection geometry is:

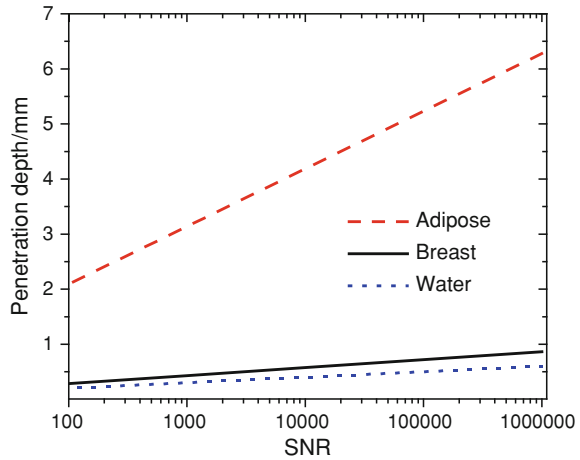
$$d = \frac{1}{\alpha} \ln(\text{SNR}) \quad (16.6)$$

Figure 16.4 illustrates how the penetration depth increases with SNR for water, breast tissue, and adipose tissue at 1 THz for reflection geometry. Since adipose tissue has a much lower attenuation coefficient than water (at 1 THz it is 25 cm^{-1} compared to 225 cm^{-1}), the terahertz light can penetrate much deeper in adipose tissue than in water or breast for a given SNR. This is particularly relevant for the application to breast cancer as the healthy tissue within the breast is largely composed of adipose tissue: if terahertz imaging were performed during surgery, it could potentially be used to look through the adipose tissue for remaining tumour.

16.3.5 Structural Versus Spectroscopic Information

Clearly, the spectroscopic information that can be obtained is dependent on the usable bandwidth of the system. The bandwidth and SNR also affect the time-domain properties of the THz signal as they also influence the axial resolution and penetration depth. The axial resolution and penetration depth determine the capability of the THz system to resolve and identify structural features. For instance, the separation between two reflections in the time-domain response can be used to calculate the thickness of a material.

Fig. 16.4 Penetration depth in adipose tissue (*dashed line*), breast tissue (*solid line*), and water (*dotted line*) as a function of SNR at 1 THz



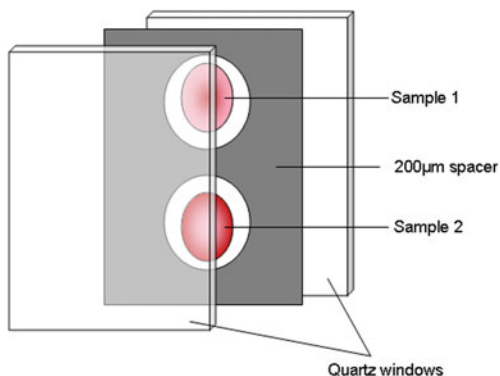
16.3.6 Imaging Versus Spectroscopy

The term THz spectroscopy is used typically when only the frequency dependent properties are of interest. A lot of spectroscopy measurements hitherto have been carried out in transmission geometry as it is easier to extract the properties more accurately. Reflection spectroscopy is becoming increasingly popular as it is often easier for sample preparation although extracting the optical properties is not quite as easy. THz imaging refers to when an image of a sample is taken—this means that data will have been recorded at several points over the sample. This can be done in either transmission or reflection geometry. The time-domain data acquired for the image can also be Fourier transformed to determine the spectroscopic information (as long as suitable acquisition parameters were chosen), though often it is the time-domain properties that are plotted to obtain the image.

16.4 Sample Holders and Effects on Calculations

While measuring biological samples great care needs to be taken to both protect the sample and to keep equipment hygienic. Below are some suggested sample holder geometries, preparation, and measurement tips for transmission and reflection geometry setups.

Fig. 16.5 Schematic diagram showing a sample holder for transmission measurements. The two quartz windows sandwich a 200 μm spacer. The spacer has holes cut so that samples can be placed between the windows to give a uniform sample thickness



16.4.1 Transmission Geometry

Since thin samples are used in transmission geometry, the sample holder should be designed to minimize dehydration. Rather than placing the sample in free space over an aperture, it is better to contain the sample between non-porous windows. This will better preserve the sample and it will also keep the thickness of the sample more uniform. A suggested setup is illustrated in Fig. 16.5.

The windows of the sample holder must be transparent to THz light and it is helpful for them to be transparent at visible frequencies too. Examples of materials that are suitable are *z*-cut quartz, TPX (poly 4 methyl pentene-1), polyethylene, and topas. Quartz is used as an example in Fig. 16.5. The spacer should also be made from a non-porous and incompressible material so that when the windows are pressed against the spacer, the sample will have a uniform thickness. It can be quite tricky cutting biological samples to an appropriate shape and thickness. In this setup, the samples need to be approximately 200 μm thick, but if slightly thicker, they can be shaped to be the thickness of the spacer by gently pressing them between the quartz windows. However, the more rigid the sample is, the more accurate the sample needs to be cut in the first place. If the windows are pressed together with too much force, they may crack (particularly if using quartz) and so it is often more economical to use plastic windows such as TPX.

For the sample measurement, the signal having passed through the windows and the sample is recorded. In order to extract the spectroscopic properties from the sample, a reference measurement is needed. In Fig. 16.6, two alternative geometries are given for the reference measurement. Fig. 16.6a has the same setup as for the sample measurement except with no sample, so there is effectively an air gap (of the same thickness as the sample) between the windows. Fig. 16.6b uses the same windows but places them together without the spacer (and without the sample). This method is preferred over Fig. 16.6a because it reduces etalon effects. The reader is encouraged at this point to think how the calculation of the refractive index and absorption coefficient will be affected by the two geometries (consider the Fresnel

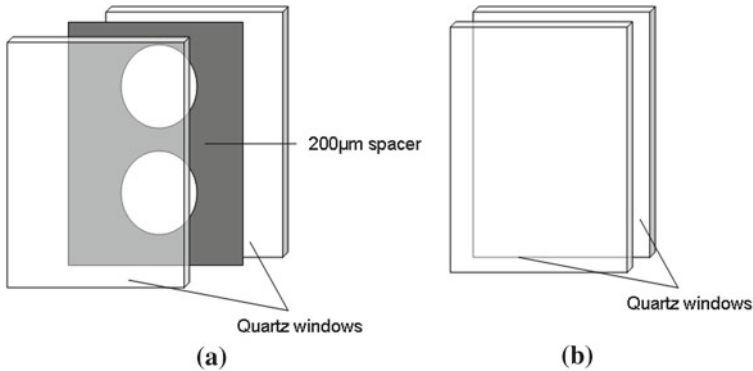


Fig. 16.6 Sample holder set ups for reference measurements. In **a** the quartz windows sandwich the spacer with no sample present. In **b** the two windows are placed together with no spacer present

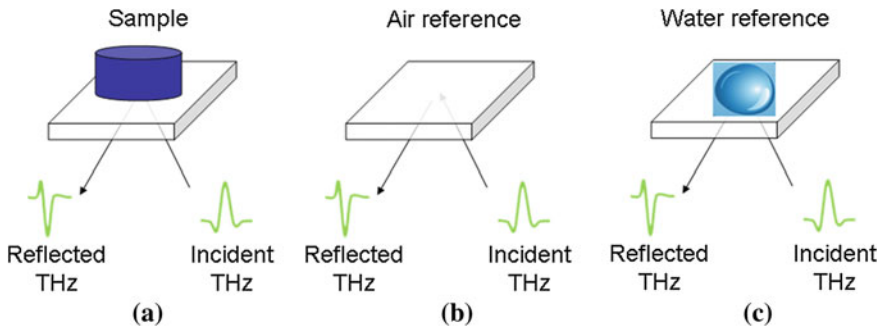


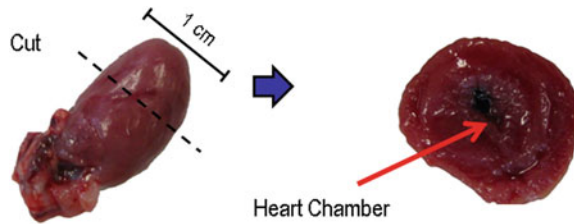
Fig. 16.7 Schematic diagrams to illustrate the sample **(a)** and reference **(b)** and **(c)** measurements used to extract the refractive index and absorption coefficient of the sample in reflection geometry

reflections at each interface). The corresponding equations for this setup can be found in reference [4].

16.4.2 Reflection Geometry

For reflection geometry, the sample preparation is easier as a thick slice of tissue should be placed on the quartz window as illustrated in Fig. 16.7a. One drawback of reflection geometry measurements is that unwanted reflections may result. For instance, reflections of the lower surface of the quartz may have an enduring effect that then interferes with the main sample reflection. One way to overcome this is to also take a measurement of water. Since the THz properties of both air and water are known, the contribution from unwanted reflections can be calculated. The derivation and equations for this are given in reference [5].

Fig. 16.8 Photograph of the heart sample illustrating how it was cut for the measurement



16.5 Interpreting Data in the Time Domain

16.5.1 Deconvolution

The incident THz signal is dependent on the various components of the THz system and particularly the photoconductive devices. Therefore, it is useful to remove the response of the incident THz signal and to determine the sample response function. This can be done by a simple deconvolution. Equation 16.7 below summarizes this process.

$$\text{Sample Response Function} = \text{FFT}^{-1} \left(\frac{\text{FFT}(\text{Sample})}{\text{FFT}(\text{Reference})} \times \text{FFT}(\text{Filter}) \right) \quad (16.7)$$

In this process, the sample is divided by the reference in Fourier space. This can create more noise, and so a filter is applied. Typically, a band pass filter such as a double Gaussian filter is chosen so as to remove both the high and low frequency noise. The resulting sample response function is in the time domain and is often used to construct an image of the sample.

16.5.2 Worked Example

A heart excised from a rat was sliced and then imaged—THz reflection measurements were taken over a 1 cm by 1 cm area by scanning the THz optics. The section of the heart placed on the quartz window contained part of the heart chamber. Figure 16.8 is a photograph of the sample before and after cutting it for the measurement.

Figure 16.9a is a schematic diagram of the sample measurement setup and Fig. 16.9b is the resulting THz image. The image was formed by plotting the maximum electric field in the sample response function at each point. The three sample response functions depicted in Fig. 16.9c are very different—the response function from the area around the sample (A) has a positive peak (it is due to the reflection of the quartz/air interface). The response function from the heart chamber area has a peak and then a trough because the incident signal passes through an air gap before

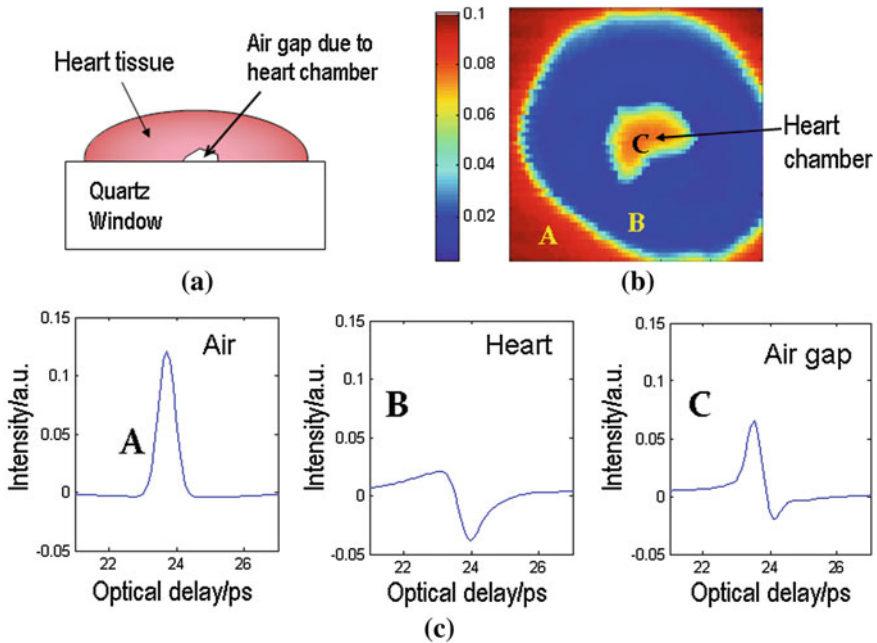


Fig. 16.9 **a** Schematic diagram of sample measurement highlighting the air gap due to the sample chamber; **b** THz image of the heart tissue section, the maximum electric field of the response function is plotted according to the color bar; **c** resulting response functions from the air at the edge of the sample (A), the heart tissue (B) and the heart chamber (C)

then being reflected of the heart chamber wall. The response function that is from the heart tissue (with no air gap) gives a trough as there are no other layers present to cause a peak. Thus, by plotting the maximum electric field from the response functions on a false color scale, the heart chamber can be seen. The refractive index and absorption coefficient of the heart tissue can be calculated through reflection spectroscopy if the sample response functions from the heart tissue (without an air gap, i.e. from area B) are used as detailed in [6].

16.6 Medical Applications Investigated

The previous sections have discussed the motivation and methods for investigating the THz properties of biomedical samples. In this section, applications that have been investigated hitherto will be outlined. More examples and details can be found in previously published review papers [7–9].

16.6.1 Breast Cancer

Ex vivo studies of breast cancer have been able to detect tumor that is of the non-calcified form [10]. This is particularly significant because such tumors are often missed during breast surgery as they are non-palpable and do not show up on X-ray images. Because of this finding, researchers are keen to develop the technique such that THz imaging can be used by clinicians intraoperatively. To determine the feasibility of such a technique, the fundamental THz properties (the absorption coefficient and refractive index) of the constituent tissues within the breast have been measured in transmission spectroscopy [11]. The results are promising—the healthy adipose tissue has a low absorption coefficient such that for an SNR of 1000, tumour buried beneath about 3 mm of adipose tissue could be detected.

16.6.2 Skin Cancer

THz images of skin cancer, namely basal cell carcinoma (BCC) have shown contrast between diseased and healthy tissues [12]. Since THz is able to penetrate the topmost layer of skin, it is possible to see the extent of the tumor beneath the surface—this cannot be seen with the naked eye, nor easily imaged with other existing modalities. The contrast in THz images of skin cancer is due to differences in the fundamental THz properties of the tissues. The refractive index and absorption coefficient of BCC are higher than healthy skin from the same patient [13]. The difference in these properties has been attributed to changes in water content and structural changes caused by increased vascularity and blood flow around the tumor. Simulation work has been conducted to further understand the contrast mechanisms [14, 15]. Recent studies have shown that structural changes contribute more than water content changes for the case of liver cirrhosis [4].

16.6.3 Colon Cancer

THz images of ex vivo colon tissue have been able to distinguish between normal colon, tumor, and even dysplastic tissue [16]. Although this pilot study was conducted ex vivo, with advances in THz wave-guiding and fiber-coupled THz devices, a THz endoscope could be possible in the future.

16.6.4 Dental Caries

The potential of THz imaging to monitor tooth decay was studied by Crawley et al. [17]. They showed that THz light could detect regions of tooth decay (caries) in excised teeth samples. Dentists were interested in the ability of the technique to detect early tooth decay using a non-ionizing imaging modality. Pickwell et al. continued the study to investigate the correlation between mineral content lost and the THz refractive index profile as a function of depth into the enamel [18]. A comparison between THz and transmission microradiography measurements was conducted for samples carefully prepared such that the lesions were in one of four groups:

1. deep with high mineral loss
2. shallow with high mineral loss
3. deep with low mineral loss
4. shallow with low mineral loss

where deep/shallow refers to the depth of decay into the enamel (parameter d in Fig. 16.10b). The extent of mineral loss is represented by parameter R in Fig. 16.10b— R is larger for higher mineral loss. Transmission microradiography is able to measure the mineral content quantitatively as the minerals block the X-rays, however, the sample is cut into $5\ \mu\text{m}$ slices for the measurement and is thus destroyed. The mineral density of the enamel is higher in the inner enamel and decreases approaching the surface. The change in mineral content causes a change in refractive index and this gives rise to two reflections in the response function illustrated in Fig. 16.10a. The distance between the reflections is related to the depth of the enamel decay (d).

The greater the change in THz refractive index between the healthy enamel and the decayed enamel, the greater the parameter R in Fig. 16.10b. This also makes the THz reflections stronger and so shallow lesions (i.e. lesions with a small parameter d in Fig. 16.10b) could still be resolved. However, if both the mineral loss was low and the depth of decay was shallow, it was no longer possible to detect the lesion [19].

16.6.5 Skin

The aforementioned applications were *ex vivo* studies. Very few *in vivo* THz studies have been conducted to date. However, there have been some studies of human skin *in vivo*. Since skin is easily accessible, reflection geometry *in vivo* THz measurements can be made to determine information about the skin such as its moisture content [20] or thickness [21]. As illustrated in Fig. 16.11b the outer layer of the skin is called the stratum corneum and beneath the stratum corneum lies the epidermis. The stratum corneum ranges from about 10 to 200 μm thick depending on the location of the skin. For instance on the wrist it is about 10–20 μm thick, whereas on the palm of the hand it is about 100–200 μm and varies a lot from person to person. TeraView

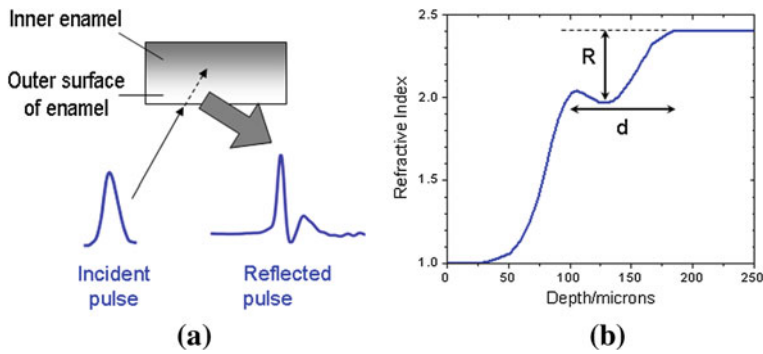


Fig. 16.10 **a** A cross-section of the tooth sample showing the THz reflections arising from enamel. The enamel has lower mineral density in areas of decay, and so there is a gradient of mineral content with the mineral content being lowest on the outer surface of the enamel. **b** The refractive index profile calculated from the reflected pulse. Label *d* marks the depth of the decay into the tooth and label *R* indicates the change in refractive index

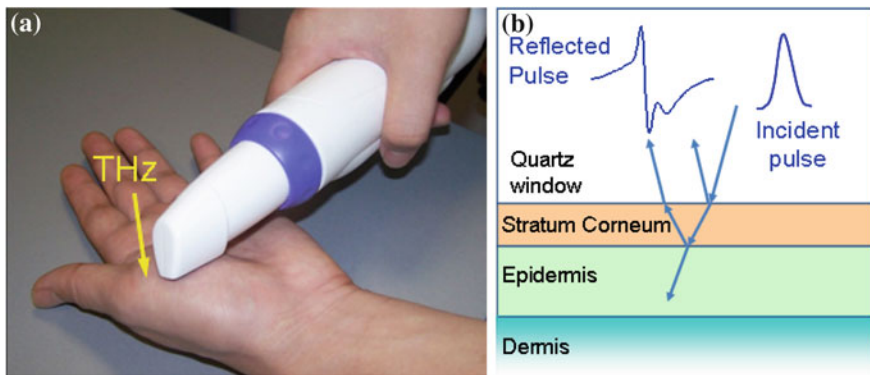


Fig. 16.11 **a** Photograph of the THz probe being used to image the palm; **b** schematic diagram showing the layers of the palm and the resulting reflected THz response function

Ltd Cambridge has designed a handheld THz probe that can be easily used (from a geometry point of view) to measure patients. We have used it to measure human skin *in vivo* to test its capabilities.

We have also shown that THz imaging can potentially be used to look through wound dressings. In our feasibility study, we were still able to determine the optical delay between the stratum corneum and epidermis when the palm was covered with a Tegaderm[®] plaster [22]. Other work along these lines includes THz imaging of porcine skin burns beneath cotton gauze [23].

16.6.6 Protein Spectroscopy

Since THz is sensitive to intermolecular interactions, THz spectroscopy can be used to characterize proteins. This could be useful for diagnosis where the presence of a particular biomarker protein is indicative of disease for example tryptophan [24] and antibodies [25]. THz spectroscopy is sensitive to small changes in molecular structure and concentrations of proteins, and thus has great potential in this area. Spectroscopy of proteins and their interactions with liquids such as water and glycerol is discussed further in (Chap. 3.2).

16.7 Summary

In summary, THz imaging uses non-ionizing radiation at low power levels and is safe to use in biomedical applications. Its great sensitivity to subtle changes in molecular structures gives THz spectroscopy the potential to be a powerful tool for medical diagnosis, be it detecting macroscopic changes in biological tissues or changes in protein concentration in solutions. However, to achieve meaningful results, careful and consistent sample preparation, sample measurement, and data analysis must be performed.

References

1. R.H. Clothier, N. Bourne, Effects of THz exposure on human primary keratinocyte differentiation and viability. *J. Biol. Phys.* **29**, 179–85 (2003)
2. O. Zeni, G.P. Gallerano, A. Perrotta, M. Romano, A. Sannino, M. Sarti et al., Cytogenetic observations in human peripheral blood leukocytes following in vitro exposure to THz radiation: a pilot study. *Health Phys.* **92**, 349–57 (2007)
3. S. Sy, S. Huang, Y.-X.J. Wang, J. Yu, A.T. Ahuja, Y. Zhang, E. Pickwell-MacPherson, Terahertz spectroscopy of liver cirrhosis: investigating the origin of contrast. *Phys. Med. Biol.* **55**, 7587–7596 (2010)
4. P.C. Ashworth, E. Pickwell-Macpherson, E. Provenzano, S.E. Pinder, A.D. Purushotham, M. Pepper, and V.P. Wallace, *Opt. Express* **17**, 12444 (2009).
5. S. Huang, P.C. Ashworth, K.W.C. Kan, C. Yang, V.P. Wallace, Y. Zhang, E. Pickwell-MacPherson, Improved sample characterization in terahertz reflection imaging and spectroscopy. *Opt. Express* **17**(5), 3848–3854 (2009)
6. S.Y. Huang, Y.X. Wang, K.W. Yeung, A.T. Ahuja, Y.-T. Zhang, E. Pickwell-MacPherson, Tissue characterisation using terahertz pulsed imaging in reflection geometry. *Phys. Med. Biol.* **54**, 149–160 (2009)
7. E. Pickwell, V.P. Wallace, Biomedical applications of THz technology. *J. Phys. D Appl. Phys.* **39**, R301–R310 (2006)
8. E. Pickwell-MacPherson, V.P. Wallace, Terahertz pulsed imaging—a potential medical imaging modality? *Photodiagn. Photodyn. Ther.* **62**, 128–134 (2009)
9. E. Pickwell-MacPherson, Practical considerations for in vivo THz imaging. *J. Terahertz Sci. Technol.* **3**(4), 163–171 (2010)

10. A.J. Fitzgerald, V.P. Wallace, M. Jimenez-Linan, L. Bobrow, R.J. Pye, A.D. Purushotham, D.D. Arnone, Terahertz pulsed imaging of human breast tumors. *Radiology* **239**, 533–540 (2006)
11. P.C. Ashworth, E. Pickwell-MacPherson, S.E. Pinder, E. Provenzano, A.D. Purushotham, M. Pepper, V.P. Wallace, Terahertz pulsed spectroscopy of freshly excised human breast cancer. *Opt. Express* **17**(15), 12444–54 (2009)
12. V.P. Wallace, A.J. Fitzgerald, S. Shankar, N. Flanagan, R. Pye, J. Cluff, D.D. Arnone, Terahertz pulsed imaging of basal cell carcinoma ex vivo and in vivo. *Br. J. Dermatol.* **151**, 424–432 (2004)
13. V.P. Wallace, A.J. Fitzgerald, E. Pickwell, R.J. Pye, P.F. Taday, N. Flanagan, T. Ha, Terahertz pulsed spectroscopy of human basal cell carcinoma. *J. Appl. Spectrosc.* **60**(10), 1127–1133 (2006)
14. E. Pickwell, B.E. Cole, A.J. Fitzgerald, V.P. Wallace, M. Pepper, Simulation of terahertz pulse propagation in biological systems. *Appl. Phys. Lett.* **84**(12), 2190–2192 (2004)
15. E. Pickwell, V.P. Wallace, A.J. Fitzgerald, B.E. Cole, R.J. Pye, T. Ha, M. Pepper, Simulating the response of terahertz radiation to human skin using ex vivo spectroscopy measurements. *J. Biomed. Opt.* **10**(6), 064021-1–064021-7 (2005)
16. V.P. Wallace, Terahertz imaging detects cancerous tissue. SPIE Newsroom, 16 Dec 2008. <http://spie.org/x32216.xml?ArticleID=x32216>
17. D.A. Crawley, C. Longbottom, B.E. Cole, C.M. Ciesla, D. Arnone, V.P. Wallace, M. Pepper, Terahertz pulse imaging: a pilot study of potential applications in dentistry. *Caries Res.* **37**, 352–359 (2003)
18. E. Pickwell, V.P. Wallace, B.E. Cole, S. Ali, C. Longbottom, R. Lynch, M. Pepper, A comparison of terahertz pulsed imaging with transmission microradiography for depth measurement of enamel demineralisation in vitro. *Caries Res.* **41**(4955), 2007 (2007)
19. E. Pickwell-MacPherson, S.Y. Huang, Y. Sun, W.C. Kan, Y.T. Zhang, Terahertz image processing methods for biomedical applications. in *Annual International Conference of the IEEE Engineering in Medicine and Biology Society*, Vancouver 2008
20. B.E. Cole, R.M. Woodward, D. Crawley, V.P. Wallace, D.D. Arnone, M. Pepper, Terahertz imaging and spectroscopy of human skin, in vivo. *SPIE Proc.* **2001**(4276), 1–10 (2001)
21. E. Pickwell, B.E. Cole, A.J. Fitzgerald, M. Pepper, V.P. Wallace, In vivo study of human skin using pulsed terahertz radiation. *Phys. Med. Biol.* **49**, 1595–1607 (2004)
22. S.Y. Huang, E. Pickwell-MacPherson, Y.T. Zhang, *A Feasibility Study of Burn Wound Depth Assessment Using Terahertz Pulsed Imaging* (IEEE-EMBS International Summer School and Symposium on Medical Devices and Biosensors, Cambridge, 2007)
23. Z.D. Taylor, R.S. Singh, M.O. Culjat, J.Y. Suen, W.S. Grundfest, H. Lee, E.R. Brown, Reflective terahertz imaging of porcine skin burns. *Opt. Lett.* **33**(11), 1258–60 (2008 Jun 1)
24. C.S. Joseph, A.N. Yaroslavsky, M. Al-Arashi, T.M. Goyette, J.C. Dickinson, A.J. Gatesman, B.W. Soper, C.M. Forgione, T.M. Horgan, E.J. Ehasz, R.H. Giles, W.E. Nixon, Terahertz spectroscopy of intrinsic biomarkers for non-melanoma skin cancer. *Proc. SPIE* **7215**, 72150I (2009)
25. Y. Sun, Y. Zhang, E. Pickwell-MacPherson, Investigating antibody interactions with polar liquids using terahertz pulsed spectroscopy. *Biophys. J.* **100**(1), 225–231 (2011)